

# Predictive Modelling and Functional Group of Clay Soil Treated with Steel Slag and Calcium Carbide Residue



D. A. Ogundare<sup>1\*</sup>, O. O. Adeleke<sup>1</sup>, A. T. Akinbuluma<sup>2</sup>

<sup>1</sup>Department of Civil Engineering, University of Ilorin, Ilorin, Nigeria

<sup>2</sup>Department of Civil Engineering, Olusegun Agagu University of Science and Technology, Okitipupa, Nigeria.



**ABSTRACT:** Swell-shrink subgrade soils like clay are rich in sulphate and exhibit a high rate of volume change by swelling and shrinking during wet and dry cycles, respectively, leading to heaves, cracks, and differential settlement of pavement layers. The aim of this study was to establish predictive simulation models and functional group of clay soil treated with steel slag and calcium carbide residue. Physical and geotechnical tests (such as California bearing ratio (CBR), compaction characteristics, and consistency parameters) were carried out on the unstabilised and stabilised clay soil. Using SPSS statistical software (version 23), multiple linear regression analysis was applied to the experimental data that relate CBR to compaction parameters and additive contents (steel slag and calcium carbide residues). The generated models gave a reliable coefficient of determination,  $R^2$ , of 0.990, and 0.998, which can be used to successfully predict both unsoaked and soaked CBR of the stabilised clay soil, respectively. Fourier transform infrared spectroscopy (FTIR) analysis was examined on the clay soil, the additives, and the stabilised clay soils. The FTIR analysis showed weak peaks at 1115 and 1103  $\text{cm}^{-1}$  for all the stabilised clay soils, and this revealed that both additives drastically reduced the sulphate content in the clay soil, which consequently reduced the expansion, cracking, and disintegration rates. As a result, the clay soil's chemical bonding was enhanced through physico-chemical mechanisms.

**KEYWORDS:** Pavement layers, California bearing ratio, multiple linear regression analysis, Fourier transform infrared spectroscopy analysis, Stabilised clay soils

[Received Jul. 4, 2024; Revised Aug. 26, 2024; Accepted Sep. 1, 2024]

Print ISSN: 0189-9546 | Online ISSN: 2437-2110

## I. INTRODUCTION

Pavement failure is prevalent in Nigeria, a developing economy, with its consequent negative effects on the nation's socio-economy through fatal road accidents, loss of property, and lost travel time, amongst others. This failure is connected to a lack of adherence to mechanical performance (i.e., strength, bearing capacity, and durability) standards and an inadequate or total absence of functional group analysis of pavement construction soils (Kabeta and Lemma, 2023). When designing the thickness of flexible and rigid pavements, the California bearing ratio (CBR) is a mechanical performance test that is frequently utilised to assess soil subgrade strength while their chemical bond is determined through Fourier transform infrared spectroscopy (FTIR) analysis. However, instead of going through rigorous and time-consuming laboratory CBR experiments, generating models could be developed using relatively fewer observations in order to predict the subgrade soil properties.

Conventional additives for soil stabilisation (cement and lime), which are commonly used for improving weak subgrade soils, become problematic in sulphate-rich soils,

which often lead to cracks, heaves, and damage to overlying pavements (Kowalska *et al.*, 2023; Wang *et al.*, 2022), leading to high maintenance costs. Hence, efforts should be deepened towards harnessing alternative, cheaper materials (steel slag and calcium carbide residue) for use as stabilisers to reduce the ineffectiveness of cement and lime stabilisations in sulphate-rich soil (Adeleke *et al.*, 2020).

The American society for testing and materials (ASTM) states that improving permeability, strengthening an existing soil's strength to increase its bearing capacity to support loads, and enhancing the soil's resistance to weathering and traffic use are among the primary goals of soil stabilisation (ASTM, 2014). Utilising industrial waste materials like fly ash, silica fume, and marble dust, one can enhance the mechanical and physical characteristics of expanding soils like clay (Tanyildizi *et al.*, 2023; Mittal, 2021). Some useful correlations between the CBR of soil and the fine-grained soil's compaction and consistency parameters were generated by Rashed *et al.* (2021). The CBR value can be calculated using the successfully obtained correlation equations. In the study by Egbe *et al.* (2017), multi linear regression analysis (MLRA) was used to generate a model that links other soil properties to

\*Corresponding author: engrbamidele@gmail.com

CBR. The MLRA provides an  $R^2$  of 0.9454, making it feasible to estimate CBR at 50.9% with an error of  $\pm 3.4\%$  using the model. The use of calcium carbide residue (CCR) and ground granulated blast furnace slag (GGBS) by weight of soil increases both unsoaked and soaked CBR, according to research by Bandyopadhyay *et al.*, (2016). This suggests that higher pavement sub-base and base course thickness can be avoided. When comparing the measured and predicted lateritic soil's CBR values modified by metakaolin, an MLR design model developed by Attah *et al.*, (2019) produced an  $R^2$  of 0.9257, which makes the model useful for predicting CBR soil stabilisation.

All of these have justified why stabilising materials that are readily available locally for free or extremely inexpensive in Nigeria is necessary to increase the strength and durability of clay soil. According to the United States Geological Survey (2022), the global estimation of steel slag (SS) is between 190 and 280 million tonnes, with approximately 0.35 to 0.45 million metric tonnes produced per year in Nigeria (Akinwumi, 2014). Also, the annual production of calcium carbide residue, a by-product of the acetylene industry, amounts to about 136 million tonnes (Tang *et al.*, 2024). However, in Nigeria, gas welding workers generate 274,000 tonnes of residue from calcium carbide on an annual basis, excluding those generated from other industrial sources (Chukwudebelu *et al.*, 2013). Meanwhile, these waste materials contain heavy metals and toxic compounds that highly pollute soil and groundwater, making them hazardous to human health, the environment, and aquatic life. Hence, this research addresses their waste management and supports Sustainable Development Goals (SDGs) 1, 6, and 12, which are on no poverty, as reusing and recycling have great promise for job creation, clean water and sanitation, and responsible consumption and production, respectively.

All of these have justified why stabilising materials that are readily available locally for free or extremely inexpensive in Nigeria is necessary to increase the strength and durability of clay soil. According to the United States Geological Survey (2022), the global estimation of steel slag (SS) is between 190 and 280 million tonnes, with approximately 0.35 to 0.45 million metric tonnes produced per year in Nigeria (Akinwumi, 2014). Also, the annual production of calcium carbide residue, a by-product of the acetylene industry, amounts to about 136 million tonnes (Tang *et al.*, 2024). However, in Nigeria, gas welding workers generate 274,000 tonnes of residue from calcium carbide on an annual basis, excluding those generated from other industrial sources (Chukwudebelu *et al.*, 2013). Meanwhile, these waste materials contain heavy metals and toxic compounds that highly pollute soil and groundwater, making them hazardous to human health, the environment, and aquatic life. Hence, this research addresses their waste management and supports Sustainable Development Goals (SDGs) 1, 6, and 12, which are on no poverty, as reusing and recycling have great promise for job creation, clean water and sanitation, and responsible consumption and production, respectively.

Numerous studies have investigated the individual effects of SS (Zhang *et al.*, 2023), CCR (Zhu *et al.*, 2022), and combined effects of GGBS and CCR (Bandyopadhyay *et al.*,

2016) as soil stabilisation, with 10% SS and 30% CCR exhibiting maximum strength. However, since there is no generally acceptable standard for applying soil stabilisation (Ikeagwuani *et al.*, 2019), and to further boost the strength and resist the chemical attack of sulphate in soil stabilisation, there is a need for an optimal combination of SS and CCR, which depends on factors such as their chemical compositions, chemical bonds, and performance evaluation

In this study, the development of models through multiple linear regression for predicting the unsoaked and soaked CBR of the stabilised clay soil was examined. To investigate the physical and geotechnical properties of the clay soil as well as the stabilised clay soil, experiments were carried out. An advanced chemical test through FTIR analysis was conducted to characterise and determine the functional groups of steel slag, calcium carbide residue, clay soil, and stabilised clay soil.

## II. THEORETICAL ANALYSIS

### A. Regression Analysis

The experimental data was subjected to regression analysis using SPSS statistical software (version 23) in the form of equation 1. A statistical model was developed using multiple linear regression (MLR) analysis to assess the impact of independent variables (steel slag (SS), calcium carbide residue (CCR), maximum dry density, and optimum moisture content on the dependent variable (unsoaked and soaked CBR) of the stabilised clay soil. The strength behaviour (unsoaked and soaked CBR) of soil (unstabilised and stabilised) used in pavement construction is highly influenced by certain properties, some of which are the independent variables.

The formulation of the MLR analysis can be expressed as follows (Bevans, 2023):

$$Y = \beta_0 + \beta_1 X_1 + \beta_2 X_2 + \beta_3 X_3 + \dots + \beta_n X_n \quad (1)$$

Where, Y = is the predicted value of the dependent variable

$\beta_0$  = is the intercept

$\beta_1, \dots, \beta_n$  = is the regression coefficient for independent variables, and

$X_1, \dots, X_n$  = is the independent variables.

### B. Performance Evaluation of Regression Model

The performance criteria using Equations 2 and 3 were used to evaluate the accuracy of the model (Tran and Do, 2021).

$$RMSE = \sqrt{\frac{1}{N} \sum (O_i - P_i)^2} \quad (2)$$

$$MAE = \frac{1}{N} \sum O_i - P_i \quad (3)$$

Where,  $P_i$  is the predicted value using MLR analysis,  $O_i$  is the experimental value, and N is the number of data sets. Mean absolute error (MAE) determines the disparity between experimental and predicted values; root mean square error (RMSE) computes the square root of the disparity between predicted and experimental values. The closer the values of RMSE and MAE are to 0, the better the model fits the data and produces more accurate predictions.

### III. MATERIALS AND METHODS

#### A. Materials

The clay soil sample was collected at 1500 mm (Wilches et al., 2020; Ogunidipe et al., 2019) below the surface of the soil at latitude 70 46' 42" North and longitude 40 29' 45" East, in Osun State, Southwest Nigeria. It was brought to the laboratory and exposed to natural air for 14 days (Fatoyinbo et al., 2024) before being used. Steel slag samples were taken from Prism Steel Mills Nigeria Limited, in Osun State, Nigeria, and dried under natural air for about 12 months (Trinh, 2022; Wang et al., 2010) to reduce free lime and volume expansion (Trinh, 2022). It was classified as low-basicity slag (Sun et al., 2022) and was broken down to diminish its molecule size using a Los Angeles abrasion machine.

In Ede, Osun State, Nigeria, waste dumps produced by commercial welders were the source of CCR.

#### B. Experimental Procedure

##### I. X-Ray Fluorescence

An X-ray instrument (Phillips PW-1800) was used for XRF test to determine the chemical composition of SS and CCR in order to detect major and trace elements using X-ray fluorescence, which is enabled by the way atoms behave when they contact with radiation. The material was divided into smaller pieces and crushed to a size of less than 75 microns to create pellets, which were then placed into a sample holder on the Philips PW-1800 x-ray machine for examination (Margui et al., 2016).

##### II. Particle Size Distribution Test

Particle size distribution test is a method of separation of soils into different fractions based on the particle size. The proportions by mass of various sizes of particles present in soils are quantitatively expressed. Particle size distribution was tested following the guidelines provided in British Standard, BS 1377-2 (1990). Water was added to 1000g of air-dry clay subgrade soil in a 75 $\mu$ m sieve, washed by hand until the water was essentially clear and the remaining clay subgrade soil on the sieve was oven-dried for analysis. The dried clay subgrade soil was sieved on a mechanical sieve shaker with the largest sieve kept at the top with a cover placed on it and the receiver (pan) with no opening placed beneath the smallest sieve for about 12 minutes until the mass of soil left on each sieve remained constant.

##### III. Consistency Parameter Test

Consistency parameter test, which measured the liquid limit, plastic limit, and plasticity index, was evaluated at different SS and CCR percentages on air-dried clay soil. 500g of fine soil at different SS and CCR percentages on air-dried clay soil retained on a 425 $\mu$ m sieve was inspected in accordance with BS 1377-2 (1990). Water was added in successive stages (drier to wetter) to a small portion of the clay soil retained on a 425 $\mu$ m sieve using a grooving tool with a tip width of 2 mm to 0.25 mm. It was subjected to 25 blows close to a groove of about 13 mm in length and a drop of cup of 10 mm in the Cassagrande liquid limit apparatus. The plastic limit is described as the water content when a thread of soil being rolled shears at 3 mm in diameter (that is, the first crumbling

point or appearance of little cracks). This test was repeated for the stabilised clay soil.

#### IV. Compaction test

By determining the optimum moisture content and corresponding maximum dry density of the unstabilised clay soil and stabilised clay soils, compaction test using a standard proctor was used as stated in BS 1377-4 (1990). The standard proctor test adopted a cylindrical metal mould (proctor mould) of about 1000 cm<sup>3</sup> volume and a rammer of 2.5 kg weight with a height drop of 300 mm as the given compactive effort. Twenty-five blows were given on each layer of three, and moisture content samples were taken from the top and bottom of the mould for analysis. This test was repeated for the stabilised clay soil.

#### V. California Bearing Ratio Test

The CBR is a standard laboratory test used to determine the unstabilised and stabilised subgrade soils' strengths. Compaction test results for each individual's optimum moisture content were utilised to compact the clay subgrade soil and stabilise the clay subgrade soil in the CBR mould. The compacted soil is penetrated by the CBR machine plunger at intervals of 0.5 mm to 12.5 mm, noting the load specific to each penetration. Considering the worst conditions, the compacted clay subgrade soil and stabilised clay subgrade soil were placed in the tank for the soaked CBR test with a surcharge load of 4.5 kg. The loads at 2.5 mm and 5.0 mm penetrations were utilised to compute the CBR, as indicated by Equation 4. The detailed test procedure is provided by BS 1377-9 (1990).

$$\text{CBR (\%)} = \frac{\text{Observed load}}{\text{Standard load}} \times 100 \quad (4)$$

Where standard load at 2.5mm penetration is 13.20 kN, standard load at 5mm penetration is 20.00 kN.

#### C. Analysis of Variance

Analysis of variance (ANOVA) was used as a statistical test to determine the relationship between the independent variables (steel slag, calcium carbide residue, maximum dry density, and optimum moisture content) and the dependent variable (unsoaked and soaked CBR) based on the experimental results using SPSS (version 23).

#### D) Fourier Transform Infrared Spectroscopy Analysis

Fourier transform infrared (FTIR) spectroscopy analysis was used as an advanced analytical technique to characterise and determine the chemical functional group compositions and bonding of the clay soil, SS, CCR, and stabilised clay soil in varying contents of SS-CCR in ratios of 5:95%, 10:90%, 15:85%, and 20:80% by dry weight of clay soil. Potassium bromide (KBr) is used as a carrier and does not have any significant absorption bands that interfere with the samples in the IR spectrum to be analysed. According to Berna (2017), the grounded powdered form was pelletised using a hydraulic press, and it was then scanned in transmittance mode at a frequency range of 400cm<sup>-1</sup> and 4000cm<sup>-1</sup> using the SHIMADZU FTIR-8400S equipment as a background.

#### IV. RESULTS AND DISCUSSION

##### A) Results of X-Ray Fluorescence Analysis

The X-ray fluorescence (XRF) analysis of steel slag (SS) and calcium carbide residue (CCR) are shown in Table 1. The SS is characterised by 38.11% calcium oxide (CaO), which conforms with the findings reported by Shi (2004); Zumrawi and Babikir (2017), in which SS is between 25% and 40%, while that of CCR (68.50%) is greater and less than what was reported by Joel and Edeh (2014) (61.41%) and Quadri *et al.*, (2020) (93.74%), respectively, affirming the additives as binding and cementitious materials.

**Table 1.** Chemical composition of SS and CCR

Oxide	SS (%)	CCR (%)
SiO <sub>2</sub>	12.00	6.50
Al <sub>2</sub> O <sub>3</sub>	4.70	2.53
Fe <sub>2</sub> O <sub>3</sub>	19.40	3.23
TiO <sub>2</sub>	0.29	0.02
CaO	38.11	68.50
P <sub>2</sub> O <sub>5</sub>	2.20	0.25
K <sub>2</sub> O	0.40	7.92
MnO	12.25	0.02
MgO	0.16	0.64
Na <sub>2</sub> O	0.15	0.60
LOI	10.16	2.01

##### B. Results of engineering properties of unstabilised and stabilised clay soil

Table 2 presents the engineering properties of the clay soil (unstabilised and stabilised). Based on the unified soil classification system (USCS) ASTM D-2487 (2000), clay soil is classified as inorganic clay with high plasticity (CH), designating it as a weak subgrade material (AASHTO M145-91, 2004). The liquid limit (LL), plastic limit (PL), and plasticity index (PI) of the mix ratios decrease from 56.5 to 46.0%, 42.3 to 35.4%, and 14.2 to 10.6%, respectively. The results of the study by Abdalqadir *et al.*, (2020) and Zumrawi and Babikir (2017) also attest to these findings. The maximum dry density (MDD) decreases from 23.0 kN/m<sup>3</sup> to 18.0 kN/m<sup>3</sup> and the optimum moisture content (OMC) increases from 11.0% to 16.5%, while the strength increases from 4.9% and 2.8% to 17.1% and 15.2% in unsoaked and soaked CBR conditions, respectively. This shows an improvement in the soil's properties in terms of stiffness, strength, and stability, which is in consonance with the findings of Ogundare *et al.*, (2024). Consequently, the thickness of pavement layers (subbase and base course) varies with the CBR of the soil as it affects the cost of pavement (Ogundare *et al.*, 2018) and leads to thinner pavement layers (Saleh *et al.*, 2024). This indicates that an increase in the stabilised CBR values (unsoaked and soaked) as derived from this study will lead to a decrease in the pavement layer thicknesses, thereby reducing the cost of road construction. This further justifies that stabilising expansive soils with SS and CCR will reduce environmental consequences such as pollution of surface water, groundwater, and fertile soil and have a contribution to the green environment, as also affirmed by Kabeta and Lemma (2023).

**Table 2.** Physical and geotechnical properties of the unstabilised and stabilised clay soil

Mix ratio (%)	LL (%)	PL (%)	PI (%)	MDD (%)	OMC (%)	Unsoaked CBR (%)	Soaked CBR (%)
0	56.5	42.3	14.2	23.0	11.0	4.9	2.8
5SS + 95CCR	55.0	41.5	13.5	21.5	12.5	11.0	9.0
10SS + 90CCR	51.5	39.3	12.2	20.5	13.0	15.5	10.8
15SS + 85CCR	48.0	36.3	11.7	19.0	14.5	15.6	13.2
20SS + 80CCR	46.0	35.4	10.6	18.0	16.5	17.1	15.2

##### C. Results of Model Validation

###### I. Multiple linear regression analysis

The model equations generated are represented in Equations 5 and 6 to depict the validity of the experimental unsoaked and soaked CBR values against the predicted ones, while Figures 1 and 2 present the relationship between the experimental unsoaked and soaked CBR values against the predicted ones, which was used to measure the regression model's fit to the data. The coefficient of determination ( $R^2$ ) is an efficient tool to evaluate the constructed model, where the higher the  $R^2$  (close to 1), the higher the accuracy of the regression model (Tabachnick and Fidell, 2001). Similarly, the lower the root mean square error (RMSE) and mean absolute error (MAE) values (closer to 0), the more the model fits the data well and has more precise predictions (Tran and Do, 2021). The results gotten from the model summary (Tables 3 and 4) show that  $R^2$  values for the unsoaked and soaked CBR are 0.990 and 0.998, respectively. This signifies that SS content, CCR content, OMC, and MDD contribute 99.0% and 99.8% of the effect to both the unsoaked and soaked CBR, which is an acceptable value (Pallant, 2020). Table 5 shows that the RMSE and MAE values from the generated equations are 0.259, 0.078, and 0.116, 0.006 for both unsoaked and soaked CBR, respectively. Hence, the equations successfully correlate the unsoaked and soaked CBR values with the compaction parameters and the additives effectively. The relationship of experimental unsoaked and soaked CBR values against the predicted ones (Figures 1 and 2) indicates that they are statistically significant ( $R^2 = 0.9903$  and  $0.9983$ ) and therefore imply that experimental unsoaked and soaked CBR and the predicted ones are equivalent, justifying the model as reliable and excellent (Pellinen, 2001).

**Table 3.** Model summary for clay soil (unsoaked CBR)

Model	R	R Square	Adjusted R Square	Std. Error of the Estimate	Durbin-Watson
1	.995	.990	.982	.6350608	2.088

**Table 4.** Model summary for clay soil (soaked CBR)

Model	R	R Square	Adjusted R Square	Std. Error of the Estimate	Durbin-Watson
1	.999	.998	.986	.2815676	2.332

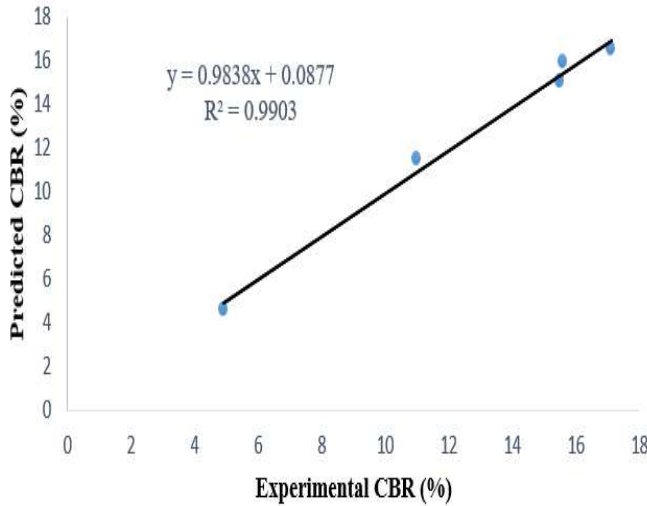


**Figure 1:** Relationship between experimental and predicted unsoaked CBR values for stabilised clay soil

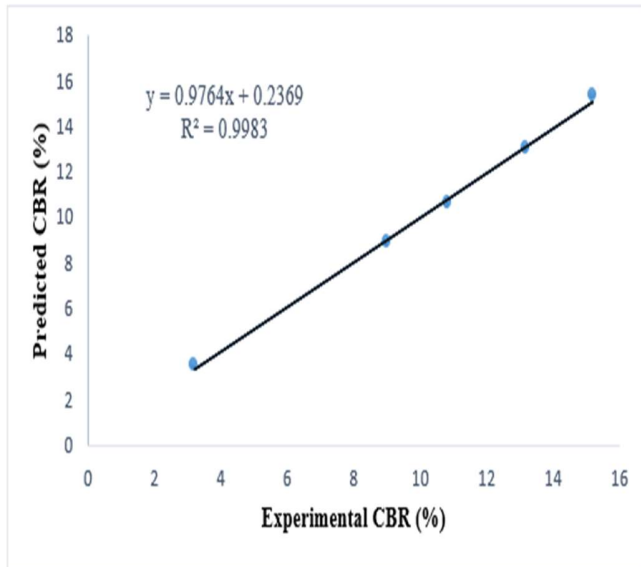


**Figure 2:** Relationship between experimental and predicted soaked CBR value for stabilised clay soil.

**Table 5.** Performance evaluation of multiple linear regression model

Equations	R <sup>2</sup>	RMSE	MAE
UCBR = 11.061 + 0.981SS + 0.056CCR - 1.721OMC + 0.543MDD	.990	.259	.116
SCBR = 11.085 + 0.229SS + 0.031CCR + 0.400OMC - 0.523MDD	.998	.078	.006

*III. Estimation of model coefficients*

From Table 6, the unstandardised coefficients for SS content, CCR content, OMC, and MDD are 0.981, 0.056, -1.721, and 0.543. This implies a strong linear positive trend within SS content and unsoaked CBR, CCR content and unsoaked CBR, maximum dry density and unsoaked CBR, and a significant linear negative relationship between optimum moisture content and unsoaked CBR. For every increase in percentages of SS content, CCR content, and unit increase in maximum dry density, the unsoaked CBR increases by 0.981%, 0.056%, and 0.543 kN/m<sup>3</sup> (adjusted b = 0.981; 95% CI 0.505,1.456; p = 0.003); (adjusted b = 0.056; 95% CI 0.031,0.081; p = 0.002); (adjusted b = 0.543; 95% CI -1.760,2.846; p = 0.571), while for every increase in percentage optimum moisture content, there is a 1.721% decrease in the unsoaked CBR (adjusted b = -1.721; 95% CI -3.298,-0.143; p = 0.038). Also from Table 7, the unstandardised coefficients for SS content, CCR content, OMC, and MDD are 0.229, 0.031, 0.400, and -0.523. This imply a strong linear positive trend within SS content and soaked CBR, CCR content and soaked CBR, optimum moisture content and soaked CBR and a significant linear negative relationship between MDD and soaked CBR. For every increase in percentages of SS content, CCR content, and OMC, the soaked CBR increases by 0.229%, 0.031%, and 0.400% (adjusted b = 0.229; 95% CI 0.063,0.395; p = 0.016); (adjusted b = 0.031; 95% CI 0.021,0.040; p = 0.000); (adjusted b = 0.400; 95% CI -0.344,1.144; p = 0.225); while for every unit increase in maximum dry density, the soaked CBR decreases by -0.523 kN/m<sup>3</sup> (adjusted b = -0.523; 95% CI -1.036, -0.010; p = 0.047).

**Table 6.** Coefficients for clay soil (unsoaked CBR)

Model	Unstandardized Coefficients		Standardized Coefficients		95.0% Confidence Interval (CI) for B		
	B	Std. Error	Beta	t	Sig.	Lower Bound	Upper Bound
Constant	11.061	24.731		.447	.673	-52.511	74.633
SS_Content	.981	.185	1.563	5.300	.003	.505	1.456
CCR_Content	.056	.010	.449	5.813	.002	.031	.081
OMC	-1.721	.614	-.723	-2.804	.038	-3.298	-.143
MDD	.543	.896	.211	.606	.571	-1.760	2.846

**Table 7.** Coefficients for clay soil (soaked CBR)

Model	Unstandardized Coefficients		Standardized Coefficients		95.0% Confidence Interval (CI) for B		
	B	Std. Error	Beta	t	Sig.	Lower Bound	Upper Bound
Constant	11.085	6.989		1.586	.174	-6.880	29.049
SS_Content	.229	.065	.400	3.551	.016	.063	.395
CCR_Content	.031	.004	.266	8.384	.000	.021	.040
OMC	.400	.289	.185	1.383	.225	-.344	1.144
MDD	-.523	.200	-.237	-2.619	.047	-1.036	-.010

The model equation generated is represented in Eqn. 5:

$$UCBR = 11.061 + 0.981SS + 0.056CCR - 1.721OMC + 0.543MDD \quad (5)$$

Where,

UCBR is the unsoaked CBR of the clay soil (%),  
 SS is the steel slag content (%),  
 CCR is the calcium carbide residue content (%),  
 OMC is the optimum moisture content of the soil (%) and  
 MDD is the maximum dry density of the soil sample (kN/m<sup>3</sup>)

The model equation generated is represented in Eqn. 6:

$$SCBR = 11.085 + 0.229SS + 0.031CCR + 0.40MC - 0.523MDD \quad (6)$$

Where,

SCBR is the soaked CBR of the clay soil (%),  
 SS is the steel slag content (%),  
 CCR is the calcium carbide residue content (%),  
 OMC is the optimum moisture content of the soil (%) and  
 MDD is the maximum dry density of the soil sample (kN/m<sup>3</sup>)

### III. Analysis of variance of the selected parameters

ANOVA was used to ascertain the suitability of the proposed model and whether or not the independent variables contributed to the regression model by determining their statistical significance (Sig). The results of the ANOVA in Tables 8 and 9 confirm that SS content, CCR content, OMC, and MDD statistically significantly predict the unsoaked and soaked CBR,  $F(4, 5) = 120.695, p(.000) < .05$  and  $F(4, 5) = 517.356, p(.000) < .05$ .

Table 8. ANOVA for Clay Soil (Unsoaked CBR)

Model	Sum of Squares	df	Mean Square	F	Sig.
1 Regression	194.706	4	48.676	120.695	.000
Residual	2.017	5	.403		
Total	196.723	9			

Dependent Variable: Unsoaked\_CBR

Predictors: (Constant), MDD, CCR\_Content, OMC, SS\_Content

Table 9. ANOVA for Clay Soil (Soaked CBR)

Model	Sum of Squares	df	Mean Square	F	Sig.
1 Regression	164.064	4	41.016	517.356	.000
Residual	.396	5	.079		
Total	164.461	9			

Dependent Variable: Soaked\_CBR

Predictors: (Constant), MDD, CCR\_Content, OMC, SS\_Content

### D. Results of Fourier Transform Infrared (FTIR) spectroscopy

#### I. FTIR spectroscopy analysis of clay soil

As depicted in Figure 3 showing the FTIR spectra of clay soil sample, the presence of strong peak at 1115 cm<sup>-1</sup> indicates SO<sub>4</sub><sup>2-</sup> stretching, affirming that the clay soil sample is rich in sulphate, which causes expansion, cracking, disintegration,

and deleterious effects on the bearing capacity and strength of the clay soil (Adeleke et al., 2020). Meanwhile, sulphates have been observed to have strong peaks at 1150–1100 cm<sup>-1</sup> (Uusitalo et al., 2020). The strong peaks at 3696, 3619, and 3445 cm<sup>-1</sup> are attributed to non-bonded hydroxyl (O-H) group stretching, with a broad peak at 3445 cm<sup>-1</sup> indicating possible hydration in the soil sample (clay soil). This conforms to the investigation made by Kasprzhitskii et al., (2018). The strong peaks of O-H stretching at 3696, 3619, and 3445 cm<sup>-1</sup> show that the clay soil is hydrophilic (water-loving) in nature because it forms hydrogen bonds with water, indicating its high affinity for water. Also, absorption bands at 3696, 3619, 3445, 1034, 694, 536, and 421 cm<sup>-1</sup> indicate that the clay soil is rich in kaolinite. This is in conformity with the findings of Jozanikohan and Abarghoeei (2022). Similarly, peaks at 3619, 3445, 1034, and 536 cm<sup>-1</sup> indicate the presence of illite in the clay soil. This conforms to the study by Jozanikohan and Abarghoeei (2022); Pineau et al., (2020).

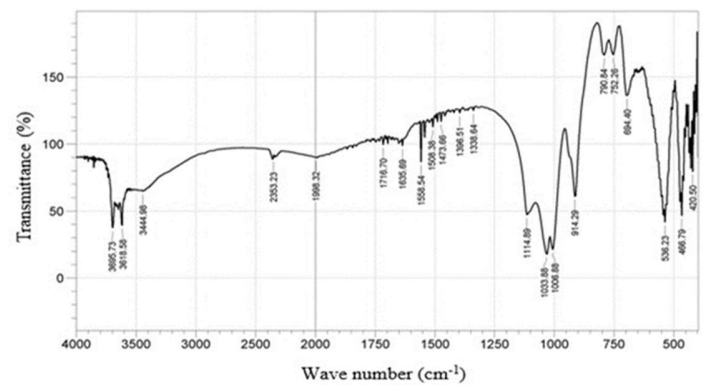


Figure 3. FTIR spectrum of clay soil

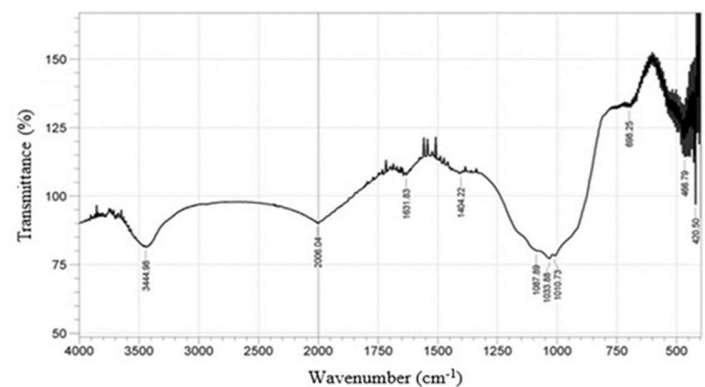


Figure 4. FTIR spectrum of steel slag

#### II. FTIR spectroscopy analysis of steel slag

The FTIR spectrum of SS, as shown in Figure 4, indicates the presence of a broad signal at 3445 cm<sup>-1</sup> indicating O-H hydrogen bonding and O-H deformation at band 1011 cm<sup>-1</sup>, affirming its low affinity for water. The presence of a weak peak at 1632 cm<sup>-1</sup> corresponds to bending O-H in hydrated phases. The band at 1034 cm<sup>-1</sup> corresponds to Si-O-Si and Si-O stretching, which indicate that SS is rich in silica, as affirmed



by García-Lodeiro *et al.*, (2009), which can lead to the formation of silicate chains with calcium-rich materials to improve the strength of soil (Wanare *et al.*, 2023).

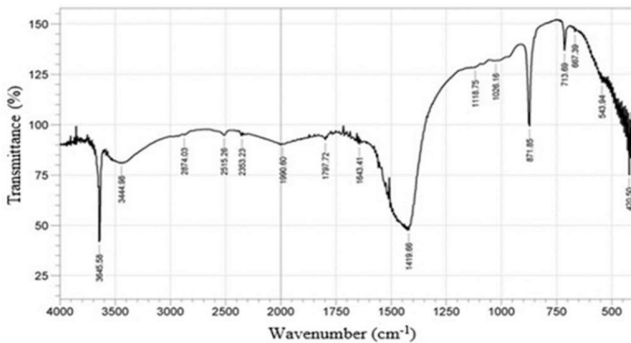


Figure 5. FTIR spectrum of calcium carbide residue

III. FTIR spectroscopy analysis of calcium carbide residue

Figure 5 shows the FTIR spectrum of CCR. A sharp peak at 3646  $\text{cm}^{-1}$  was observed, which denotes the hydroxyl group (O-H), with a broad peak at 3445  $\text{cm}^{-1}$  indicating O-H hydrogen bonding. The band at 2874  $\text{cm}^{-1}$  corresponds to the C-H group of methylene. Weak peaks at 2515  $\text{cm}^{-1}$  and 1797  $\text{cm}^{-1}$  correspond to C=O stretching of carbonates (Ismail *et al.*, 2016) and C=O of aryl carbonate, indicating the presence of calcium carbonate ( $\text{CaCO}_3$ ) in CCR. At 1420  $\text{cm}^{-1}$ , a broad peak was noticed, which corresponds to calcium oxide (CaO), signifying a high concentration of CaO in CCR. This is in line with the findings of Ajala *et al.*, (2020). The weak signal at 1643  $\text{cm}^{-1}$  is attributed to C=C of alkene.

IV. FTIR spectroscopy analysis of stabilised clay soil samples

The presence of weak peaks at 1115 and 1103  $\text{cm}^{-1}$  for all the stabilised clay soil shows that both additives drastically reduced the sulphate in the clay soil, which consequently reduced the expansion, cracking, and disintegration rate of the clay soil. Figures 6 and 7 show the spectra of the stabilised clay soil at 5% SS+95% CCR and 10% SS+90% CCR, respectively. There is an appearance of bands at 2928  $\text{cm}^{-1}$  due to C-H methyl stretching indicating traces of carbonates. Also, the stabilised clay soil at 15% SS+85% CCR as shown in Figure 8 shows an appearance of a band at 1636  $\text{cm}^{-1}$ , and at 20% SS+80% CCR as shown in Figure 9, there is an appearance of broad and strong peaks at 1636 and 1427  $\text{cm}^{-1}$  due to the C=C aromatic compound of alkene corresponding to the presence of carbonate. This is consistent with the findings reported by Pineau *et al.*, (2020), that shows that SS and CCR improved the chemical bonding of the clay soil, leading to macro aggregate stabilisation; hence, increased the strength, conjugation, and rigidity of the clay soil.

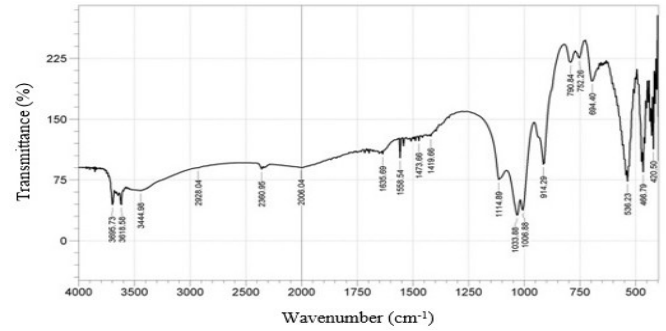


Figure 6. FTIR spectrum of clay soil stabilised with 5%SS+95%CCR

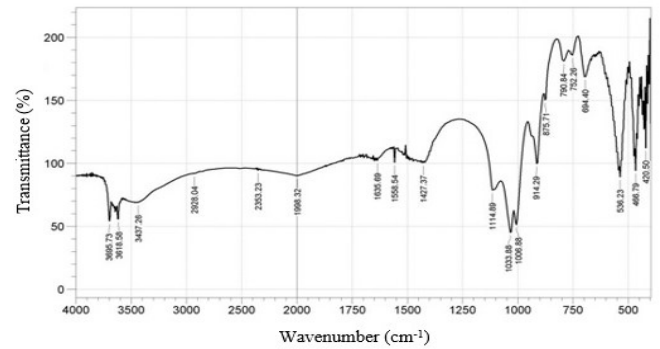


Figure 7. FTIR spectrum of clay soil stabilised with 10%SS+90%CCR

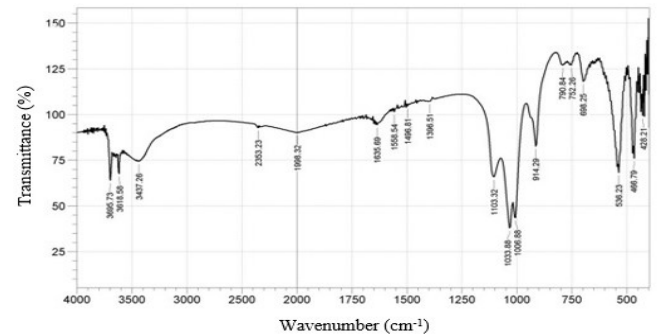
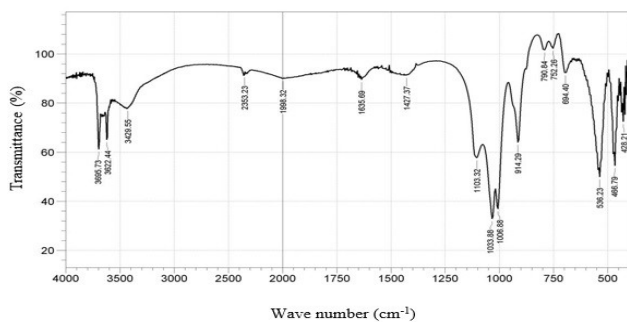


Figure 8. FTIR spectrum of clay soil stabilised with 15%SS+85%CCR



**Figure 9.** FTIR spectrum of clay soil stabilised with 20%SS+80%CCR

#### IV. CONCLUSION

The utilisation of a multiple linear regression analysis model for forecasting sulphate-rich inorganic clay soil with high plasticity using steel slag and calcium carbide residue as stabilisers has been successfully evaluated. Optimal compaction conditions (dry density and moisture content) have significant effects on the strength (California bearing ratio (CBR) values) of different soil types. The results gave a significant coefficient of determination ( $R^2$ , 99.0% and 99.8%) and high accuracy performance values of 0.259 and 0.078 for root mean square error and 0.116 and 0.006 for mean absolute error when both the unsoaked and soaked CBR were correlated with compaction parameters and the additives. This makes the multiple linear regression analysis a good and reliable regression model for estimating CBR of inorganic clay soil with high plasticity.

The band at  $1034\text{ cm}^{-1}$  which corresponds to Si-O-Si and Si-O stretching, indicates that steel slag is rich in silica, which can lead to the formation of silicate chains with calcium-rich materials to improve the strength of soil. Also, weak peaks at  $2515\text{ cm}^{-1}$  and  $1797\text{ cm}^{-1}$  corresponding to C=O stretching of carbonates and C=O of aryl carbonate reveal the presence of calcium carbonate ( $\text{CaCO}_3$ ) in calcium carbide residue, which can act as a cementing agent to improve the chemical bonding of soil. The presence of weak peaks at  $1115$  and  $1103\text{ cm}^{-1}$  for all the stabilised clay soils revealed that the steel slag and calcium carbide residue reduced the sulphate in the clay soil, which consequently reduced the expansion, cracking, and disintegration rate of pavement through physico-chemical mechanisms. These results not only confirm the viability of calcium carbide residue and steel slag in enhancing the performance evaluation of clay soil by sufficiently reducing its sulphate content but also serve as environmentally friendly materials that would help in waste management, thus addressing sustainable development and climate change.

#### AUTHOR CONTRIBUTIONS

**D. A. Ogundare:** Conceptualization, Methodology, Software, Characterisation, writing – original draft, Writing – review & editing. **O. O. Adeleke:** Supervision, Writing – review & editing. **A. T. Akinbuluma:** Methodology, Writing – review & editing.

#### REFERENCES

- AASHTO (2004).** Standard Specification for Classification of Soils and Soil-Aggregate. Mixtures for Highway Construction Purposes. American Association of State Highway and Transportation Official, AASHTO Designation: M145-91.
- Abdalqadir, Z. K.; N. B. Salih and S. J. H. Salih (2020).** Using Steel Slag for Stabilizing Clayey Soil in Sulaimani City-Iraq. *Journal of Engineering*, 26(7): 145-157.
- Adeleke, B.; J. Kinuthia and J. Oti (2020).** Strength and Swell Performance of High-Sulphate Kaolinite Clay Soil. *Sustainability*, 12(3): 10164.
- Ajala, E. O.; M. A. Ajala; A. O. Ajao; H. B. Saka and A. C. Oladipo (2020).** Calcium-Carbide Residue: A Precursor for the Synthesis of  $\text{CaO-Al}_2\text{O}_3\text{-SiO}_2\text{-CaSO}_4$  Solid Acid Catalyst for Biodiesel Production using Waste Lard. *Chemical Engineering Journal Advances*, 4: 100033.
- Akinwumi, I. I. (2014).** Soil Modification by the Application of Steel Slag. *Periodica Polytechnica Civil Engineering*, 58(4): 371-377.
- ASTM (2014).** Standards on Soil Stabilization with Admixtures. 2<sup>nd</sup> Edition, pp. 126.
- ASTM (2000).** Standard Practice for Classification of Soils for Engineering Purpose. Unified Soil Classification System, ASTM Standards D 2487-00.
- Attah, I. C.; J. C. Agunwamba; R. K. Etim and N. M. Ogarekpe. (2019).** Modelling and Predicting CBR values of Lateritic Soil treated with Metakaolin for Road Material. *ARNJ Journal of Engineering and Applied Sciences*, 14(20): 3609-3618.e
- Bandyopadhyay, T. S.; A. A. Singh; V. Pandey and J. P. Singh (2016).** Stabilization of Soil using GGBS and Calcium Carbide Residue. *International Journal of Innovative Research in Science, Engineering and Technology*, 5(9): 17023-17030.
- Berna, F. (2017).** Fourier Transform Infrared Spectroscopy (FTIR). *Encyclopedia of Geoarchaeology*, Springer, Dordrecht.
- Bevans, R. (2023).** Multiple Linear Regression, A Quick Guide. Available online at <https://www.scribbr.com/statistics/multiple-linear-regression/>. Accessed on July 2, 2024.
- BS 1377-2 (1990).** Methods of test for Soils for Civil Engineering Purposes – Part 2: Classification tests. British Standards Institution.
- BS 1377-4 (1990).** Methods of test for Soils for Civil Engineering Purposes – Part 4: Compaction-related tests. British Standards Institution.
- BS 1377-9 (1990).** Methods of test for Soils for Civil Engineering Purposes – Part 9: In-situ tests. British Standards Institution.
- Chukwudebelu, J. A.; C. C. Igwe; O. E. Taiwo and O. B. Tojola (2013).** Recovery of Pure Slaked Lime from Carbide Sludge: Case Study of Lagos State, Nigeria. *African Journal of Environmental Science and Technology*, 7(6): 490-495.
- Egbe, J. G.; D. E. Ewa; S. E. Ubi; G. B. Ikwa and O. O. Tumenayo (2017).** Application of Multilinear



Regression Analysis in Modeling of Soil Properties for Geotechnical Civil Engineering Works in Calabar South. *Nigerian Journal of Technology* 36(4): 1059-1065.

**Fatoyinbo, I. O.; S. Malomo; Y. A. Asiwaju-Bello and A. A. Bello (2024).** Effect of Multiple-Compaction on Laterite Soil: Geotechnical and Geo-Statistical Analysis. *Scientific Reports*, 14: 4067.

**García-Lodeiro, I.; D. E. Macphee; A. Palomo and A. Fernández-Jiménez (2009).** Effect of Alkalis on Fresh C–S–H Gels, FTIR Analysis. *Cement and Concrete Research*, 39(3): 147-153.

**Ikeagwuani, C. C. and Nwonu, D. C. (2019).** Emerging Trends in Expansive Soil Stabilisation: A Review. *Journal of Rock Mechanics and Geotechnical Engineering*, 11(2): 423-440.

**Ismail, S.; A. S. Ahmed; R. Anr and S. Hamdan (2016).** Biodiesel Production from Castor Oil by using Calcium Oxide derived from Mud Clam Shell. *Journal of Renewable Energy*, 1-8.

**Joel, M. and Edeh, J. (2014).** Stabilization of Ikpayongo Laterite with Cement and Calcium Carbide Waste. *Global Journal of Pure and Applied Sciences*, 20(1): 49-55.

**Jozanikohan, G. and Abarghoeei, M. N. (2022).** The Fourier Transform Infrared Spectroscopy (FTIR) Analysis for the Clay Mineralogy Studies in a Clastic Reservoir. *Journal of Petroleum Exploration Production Technology*, 12(3): 2093-2106.

**Kabeta, W. F. and Lemma, H. (2023).** Modeling the Application Steel Slag in Stabilizing Expansive Soil. *Modeling Earth Systems and Environment*, 9: 4023-4030.

**Kasprzhitskii, A.; G. Lazorenko; A. Khater and V. Yavna (2018).** Mid-Infrared Spectroscopic Assessment of Plasticity Characteristics of Clay Soils. *Minerals*, 8(5): 184.

**Kowalska, M.; B. Grzesik; Z. Adamczyk; J. Nowak and A. Konsek (2023).** Swelling of Sulfate-Bearing Soils: A Case Study of A1 Highway Pavement Failure. *Construction Materials*, Elsevier, 18: 1-16.

**Margui, E.; I. Queralt and R. V. Grieken (2016).** Sample Preparation for X-Ray Fluorescence Analysis. *Encyclopedia of Analytical Chemistry*, 1-25.

**Mittal, A. (2021).** Effect of Rice Husk Ash and Stone Dust on selecting Engineering Properties of Poor Subgrade Soil. *Jordan Journal of Civil Engineering*, 15(1).

**Ogundare, D. A.; O. O. Adeleke and A. T. Akinbuluma (2024).** Chemical and Mechanical Characterisation of Clay Soil Stabilised with Steel Slag and Calcium Carbide Waste. *Civil and Sustainable Urban Engineering*, 4(1): 55-64.

**Ogundare, D. A.; A. O. Familusi; A. B. Osunkunle and J. O. Olusami (2018).** Utilization of Geotextile for Soil Stabilization. *American Journal of Engineering Research*, 7(8): 224-231.

**Ogundipe, O. M.; J. S. Adekanmi; O. O. Akinkulore and P. O. Ale (2019).** Effect of Compactive Efforts on Strength of Laterites Stabilized with Sawdust Ash. *Civil Engineering Journal*, 5(11): 2502-2514.

**Pallant, J. (2020).** SPSS Survival Manual: A Step by Step Guide to Data Analysis using IBM SPSS. 7th Edition, Taylor & Francis Group, London.

**Pellinen, T. K. (2001).** Investigation of the use of Dynamic Modulus as an Indicator of Hot Mix Asphalt Performance. Ph.D. Thesis, Civil Engineering Department, Arizona State University, Tempe, U.S.A.

**Pineau, M.; F. Baron; M. Mathian; L. Le Deit; B. Rondeau and T. Allard (2020).** Estimating Kaolinite Crystallinity using Near-Infrared Spectroscopy. 51st Lunar and planetary Science Conference, The Woodlands, Houston, Texas, United States.

**Quadri, H. A.; O. S. Abiola; S. O. Odunfa and J. O. Azeez (2020).** Assessment of Calcium Carbide Waste and Calcined Clay as Stabilizer in Flexible Pavement Construction. *Arid Zone Journal of Engineering, Technology & Environment*, 16(1): 109-119.

**Rashed, K. A.; N. B. Salih and T. A. Abdalla (2021).** Prediction of California Bearing Ratio for Consistency and Compaction Characteristics of Fine-Grained Soils. *Al-Nahran Journal for Engineering Sciences*, 24(2): 123-129.

**Saleh, S. A.; R. S. Ismael and B. S. Abas (2024).** Effect of Soil Stabilization on Structural Design of Flexible Pavement. *Journal of Studies in Civil Engineering*, 1(1): 36-54.

**Shi, C. (2004).** Steel Slag-Its Production, Processing, Characteristics, and Cementitious Properties. *Journal of Materials in Civil Engineering*, 16(3): 230-236.

**Sun, Y. H.; M. Z. Chen; D. Y. Chen; S. Liu; X. Zhang and S. Wu (2022).** Laboratory Preparation and Performance Characterization of Steel Slag Ultrafine Powder used in Cement-Based Materials. *Sustainability*, 14(22), 14951

**Tabachnick, B. G. and Fidell, L. S. (2001).** Using Multivariate Statistics. 4th Edition, Allyn and Bacon, Boston.

**Tang, P.; A. A. Javadi and R. Vinai (2024).** Sustainable Utilisation of Calcium-Rich Industrial Wastes in Soil Stabilisation: Potential Use of Calcium Carbide Residue. *Journal of Environmental Management*, 357: 120800

**Tanyildizi, M.; V. E. Uz and I. Gokalp (2023).** Utilization of Waste Materials in the Stabilization of Expansive Pavement Subgrade: An Extensive Review. *Construction and Building Materials*, 938.

**Tran, V. Q. and Do, H. Q. (2021).** Prediction of California Bearing Ratio (CBR) of Stabilized Expansive Soils with Agricultural and Industrial Waste using Light Gradient Boosting Machine. *Journal of Science and Transport Technology*, 1(1): 1-9.

**Trinh, S. H. (2022).** Effect of Weather Aging on Volume Expansion Properties of Steel Slag. *Journal of Science and Transport Technology*, 2(3): 26-32.

**US Geological Survey (2022).** Iron and Steel Slag Data Sheet. Mineral Commodity Summaries, Reston, Virginia.

**Uusitalo, S.; T. Soudunsaari; J. Sumen; O. Haavisto; J. Kaartinen; J. Huuskonen; A. Tuikka; K. Rahkamaa-Tolonen and J. Paaso (2020).** Online Analysis of Minerals from Sulfide Ore using Near-Infrared Raman Spectroscopy. *Journal of Raman Spectroscopy*, 51(6): 978-988.

**Wanare, S.; M. Chavhan; V. Waghmare; H. Meshram; R. Dewari and T. Gulve (2023).** Effect of Fly Ash and Sodium Silicate on Soil Stabilization. *International Journal*

of *Advances in Engineering and Management*, 5(5): 1133-1139.

**Wang, Q.; J. Long; L. Xu; Z. Zhang; Y. Iv; Z. Yang and K. Wu (2022).** Experimental and Modelling Study on the Deterioration of Stabilized Soft Soil Subjected to Sulfate Attack. *Construction and Building Materials*, 346(1): 128436

**Wang, G.; Y. Wang and Z. Gao (2010).** Use of Steel Slag as a Granular Material: Volume Expansion Prediction and Usability Criteria. *Journal of Hazardous Material*, 184: 555-560.

**Zhang, Y.; T. Jiang; S. Li and W. Wang (2023).** Engineering Properties and Environmental Impact of Soil Mixing with Steel Slag applied in Subgrade. *Applied Sciences*, 13(3): 1574.

**Zhu, X.; F. Niu; L. Ren; C. Jiao; H. Jiang and X. Yao (2022).** Effect of Calcium Carbide Residue on Strength Development along with Mechanisms of Cement-Stabilized Dredged Sludge. *Materials*, 15(13): 4453.

**Zumrawi, M. M. E and Babikir, A. A. A. (2017).** Laboratory Study of Steel Slag used in Stabilizing Expansive Soil. *Asian Engineering Review*, 4(1): 1-6.